Hindawi
Adsorption Science & Technology
Volume 2022, Article ID 5059757, 14 pages
https://doi.org/10.1155/2022/5059757

Research Article

Mechanism of Gas Desorption in Coal Particles under Different Positive Pressures: Experiments and Numerical Model

Enguang Han [1,2]

[1]*China Coal Technology and Engineering Group Chongqing Research Institute, Chongqing, China*
[2]*State Key Laboratory of Gas Disaster Monitoring and Emergency Technology, Chongqing, China*

Correspondence should be addressed to Enguang Han; khan6369@163.com

Received 7 July 2022; Revised 13 September 2022; Accepted 19 October 2022; Published 3 November 2022

Academic Editor: Ming Hua

The inaccurate calculation of the gas lost is the principal cause of inaccurate determinations of the coalbed methane content via air reverse circulation sampling (ARCS). The positive pressure environment has a significant impact on gas desorption during the sampling process. To obtain the gas desorption mechanism of coal particles under positive pressure, positive pressure desorption experiments were conducted on coal samples with different particle sizes under different adsorption equilibrium pressures using a self-designed positive pressure desorption experimental device. And a positive diffusion model for coal particles was established, in which the diffusion coefficient was calculated based on the results of the positive desorption experiments. The diffusion model was then used to simulate the diffusion capacity of coal particles and compared with the test data. The results show that the responses of the positive pressure desorption and atmospheric pressure desorption to the adsorption equilibrium pressure are similar. The gas desorption velocity increases as the adsorption equilibrium pressure increases. Positive pressure can effectively inhibit gas desorption. The initial gas desorption velocity decreases as the positive pressure and coal particle size increase. Concurrently, the entire sample desorption process during ARCS can be divided into three stages: a slow desorption stage, an accelerated desorption stage, and an atmospheric desorption stage. The relationship between the diffusion coefficient and the positive pressure exhibits an exponential distribution, and the positive pressure diffusion model can describe the gas diffusion from coal particles well. The results of this study could help to establish a gas loss compensation model for the ARCS process.

1. Introduction

Obtaining accurate coalbed methane content is of great significance for coalbed methane resource evaluation and gas disaster control [1–4]. However, in recent years, the exploration and development of coalbed methane and coal mining practices have shown that the methane content measured in surface wells is lower than the actual gas content [5, 6]. The current surface well coal seam sampling technology takes a long time to collect a sample, resulting in a large amount of gas loss during the sampling period. In the past 50 years, the Barrer type has been widely used to calculate gas loss based on its solid theoretical foundation [7]. However, due to the limitations of the theoretical assumptions and human errors in practice, this method still has disadvantages. Scholars have proposed additional methods of calculating the gas loss, such as Bolt type [8], Winter type [9], and Wang type [10], which have improved the convenience and accuracy of the loss gas calculation [11, 12]. However, these methods pay more attention to the desorption data processing stage and ignore the impacts of the environmental factors on the gas loss during the transportation of the coal samples. Thus, scholars have proposed air reverse circulation sampling (ARCS) technology for surface wells. The ARCS drilling technology adopts a center sampling down the hole (DTH) hammer, a special reverse circulation drill bit, and a double wall drill pipe drilling tool system, and the drill cuttings are carried by high-pressure and high-speed air and discharged from the bottom of the hole. This method can not only be used for hard rock drilling and taking while drilling but also has the advantages of fast sampling, high precision, cleanness, and no pollution [13].

However, in the sampling process, the coal sample is in a positive pressure environment, and during the transportation of the coal samples, the coal samples collide, resulting in a reduction in the particle size [14].

The gas desorption from the coal particles is a gas transfer process in porous media, which is affected by the particle size, gas pressure, temperature, coal rank, and other factors [15, 16]. Regarding the influence of environmental pressure on the gas desorption from granular coal, more attention should be paid to the influence of a negative pressure environment on gas desorption. A negative pressure environment can cause an increase in the gas desorption kinetic parameters such as the gas diffusion rate and gas diffusion coefficient, and it can accelerate the gas desorption, so a negative pressure environment can promote gas desorption [17, 18]. In the ARCS process, the coal sample is in a positive pressure environment in an air medium, and the desorption law under a negative pressure environment is not suitable for calculating the gas lost from the coal sample during this process. Yang et al. [19] studied the sampling process from geological exploration boreholes and the gas desorption law under a positive pressure environment in a mud medium and found that the positive pressure environment of mud can effectively inhibit gas desorption from coal samples. However, little research has been conducted on gas desorption under a positive pressure environment in an air medium. The ARCS process is accompanied by a reduction in the coal particle size. Scholars have found that there is a particle size limit for granular coal, and the initial velocity of the gas emission decreases with increasing particle size. After the coal sample reaches the particle size limit, the initial velocity of the gas emission remains unchanged. The larger the particle size of the coal sample is, the smaller the kinetic diffusion parameter is, and the smaller the methane desorption rate is [20]. However, these studies on gas desorption from different particle sizes were all carried out under atmospheric pressure. The desorption of gas from coal with different particle sizes under a positive pressure environment has rarely been studied.

In this study, the gas desorption from coal particles under different positive pressures was investigated through positive pressure desorption experiments on coal samples with different adsorption equilibrium pressures and different particle sizes. The relationship between the diffusion coefficient of the coal particles and the positive was determined. A numerical model was established to predict the gas desorption from coal particles under different positive pressure environments. The results of this study could provide a basis for the establishment of a more accurate gas loss compensation model for ARCS.

2. Materials and Methodology

2.1. Sample Preparation. The blocks of anthracite used in this study were obtained from the Sihe coal mine, Jincheng, Shanxi Province, China, and the Canghai coal mine, Bijie, Guizhou Province, China (Figure 1). The physical parameters of the coal were evaluated using Chinese national standards (Table 1). The porosity of the coal is evaluated using the Chinese national standards (MT/T 918-2002 and GB/T 217-2008). The Chinese national standard (GB/T 212-2008) is used to measure the ash content (A_{ad}), volatile matter (V_{ad}), and moisture (M_{ad}). The Chinese national standard (MT/T 918-2002) is used to measure the apparent relative density (ARD_{20}^{20}), and the Chinese national standard (GB/T 217-2008) is used to measure the true relative density (TRD_{20}^{20}). The coal specimen from Canghai was ground and sieved through 1–3 mm metal sieves. The coal specimen from Sihe was ground and sieved through 1–3 mm, 3–6 mm, 10–20 mm, 20–30mm, and 30–40 mm metal sieves. Then, the coal specimen was placed in a drying oven at 377.15–383.15 K for 1 h to dehydrate. After dehydration, the prepared sample was stored in a dehydrator for later use.

2.2. Positive Pressure Desorption Test Procedure. A self-developed desorption experimental device was used to conduct the positive pressure desorption experiments (Figure 2). The device included a vacuum degassing system, constant temperature system, sorption equilibrium system, positive pressure regulation system, and desorption measurement system. The positive pressure regulation system controlled the allowable positive pressure value by adjusting the tightness of the back pressure value nut, and the adjustment range of the positive pressure value was 0–2.5 MPa. The general procedure for the positive pressure desorption test is described below:

(1) The prepared coal sample was weighed and placed in the sample canister. The void space volume in the sample canister was calibrated, and the tightness of the entire testing system was double-checked

(2) The sample cell was vacuumed. The device pipeline and coal sample canister were vacuumed until the reading of the vacuum gauge was less than 10 Pa

(3) The canister was inflated until sorption equilibrium was reached. The sample cell gas was changed via the reference cell. The pressure change of the sample cell was monitored to determine if sorption equilibrium had been reached. Only when the pressure remained unchanged at the preset pressure for 12 h could this phase end. Once the equilibrium point was reached, this phase ended and the sorption content and pressure were obtained. The preset sorption equilibrium pressures were 1 MPa, 2 MPa, 3 MPa, and 4 MPa

(4) Positive pressure desorption: back pressure values with corresponding positive pressure values (0.2 MPa, 0.5 MPa, 1 MPa, 1.5 MPa, and 2.0 MPa; a total of five different positive pressure conditions were set for the back pressure values) were installed. The back pressure value was connected to the desorption measurement system. The drainage gas gathering drum was filled with sufficient saturated salt water. The faucet at the bottom of the drainage and gas gathering drum was opened, and the reading of the electronic scale was set to zero after the water

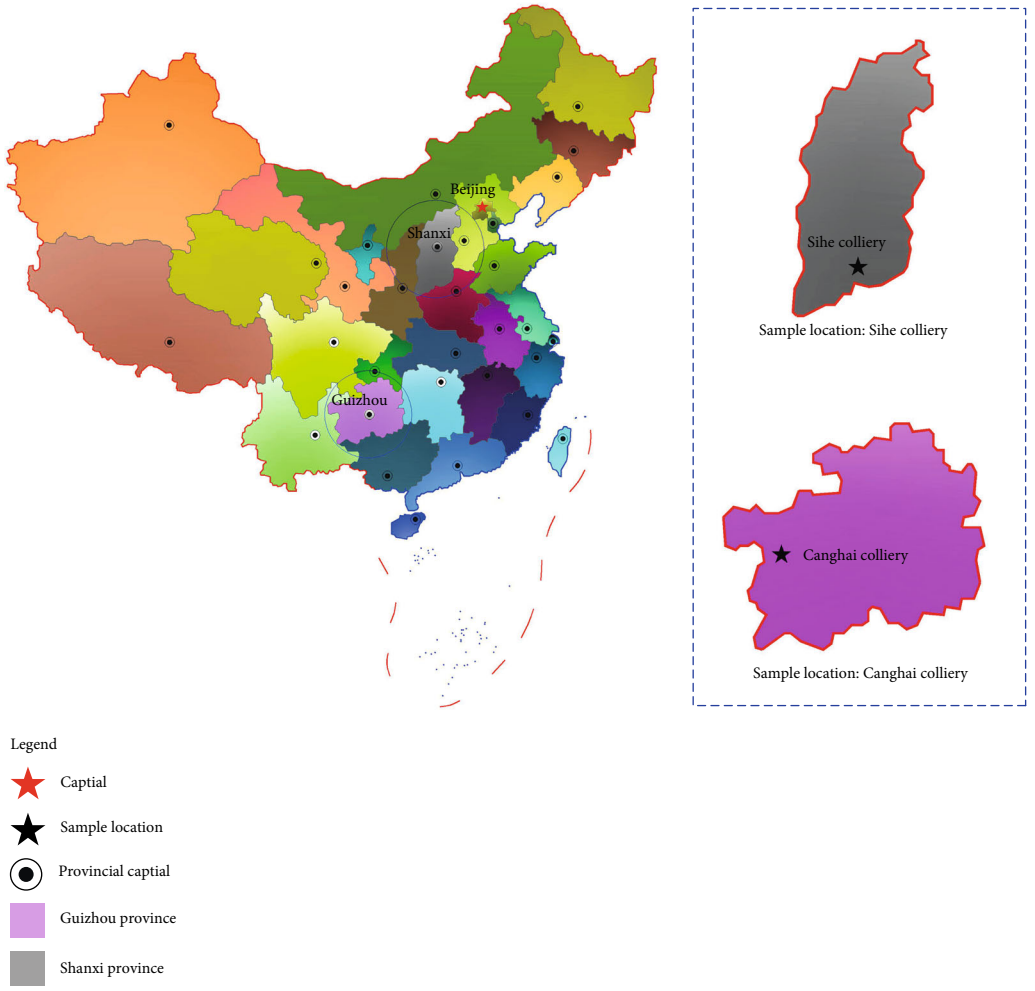

Figure 1: Geographic locations of the coal sampling sites.

Table 1: Physical parameters of the two coal samples.

Physical parameters	f value	A_{ad} (%)	V_{ad} (%)	M_{ad} (%)	TRD_{20}^{20} (g/cm^3)	ARD_{20}^{20} (g/cm^3)	Porosity (%)
Sihe	1.2	15.67	9.85	1.45	1.62	1.54	4.94
Canghai	0.24	20.91	11.17	1.58	1.75	1.66	5.14

Note: f value is called the Protodyakonov coefficient tested by the drop hammer test [21], which was developed by Russian scholar Protodyakonov and is used as one of the indexes for coal and gas outburst evaluation in China.

flow stopped. The positive pressure desorption was started, and the gas in the coal sample canister entered the drainage and gas gathering channel through the back pressure valve. The water discharge was measured using the electronic scale, and the amount of gas desorption was calculated using

$$Q = \frac{273.15 m_w}{101325(273.15 + t_w)}(p_{atm} - 9.81 h_w), \quad (1)$$

where Q is the gas desorption content under the standard state, m_w is the quantity of water discharged from the drainage gas gathering drum, p_{atm} is the atmospheric pressure, t_w is the water temperature, and h_w is the water surface height in the gas gathering drum at the end of the desorption

2.3. Method of Correcting the Free Gas Content. In the positive pressure desorption experiment, after the sample reached adsorption equilibrium, desorption began under the positive pressure environment. At this time, part of the free gas in the void space of the coal sample canister entered the drainage gas collection drum through the back pressure value, and the other parts remain in the void space. The amount of free gas in the drainage gas gathering drum was calculated by calibrating the void space and pipeline volume, and the method of collecting the free gas before desorption cannot accurately remove the free gas contained in the amount of gas desorption in the positive pressure desorption experiment.

After the experimental coal sample was loaded into the coal sample canister, the free gas content of each group of experiments was corrected. According to the extremely

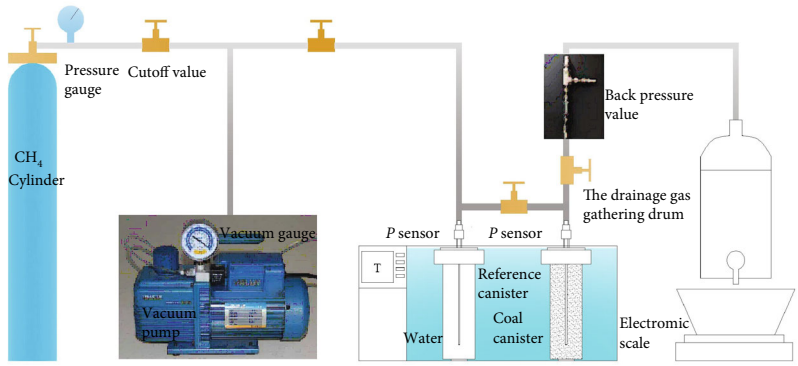

Figure 2: Desorption experiment device.

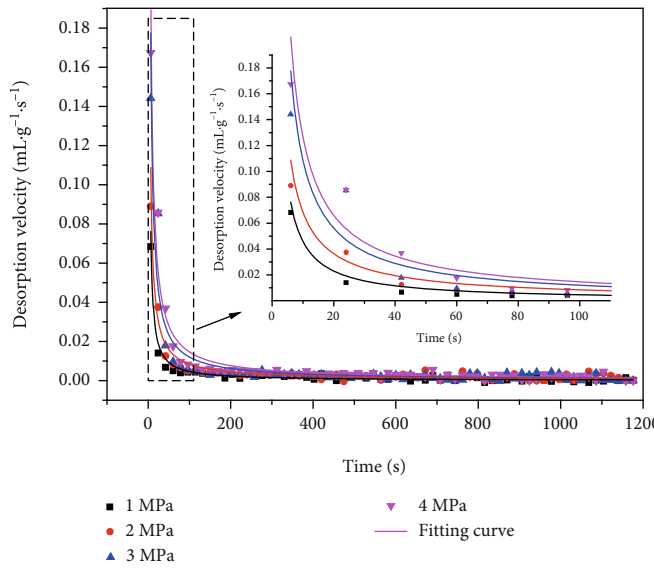

(a)

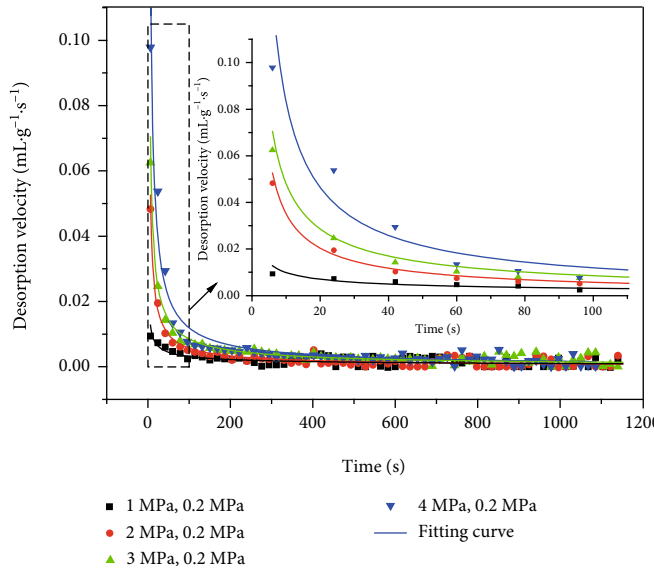

(b)

Figure 3: Relationship between desorption velocity and time: (a) under atmospheric pressure and (b) under a positive pressure of 0.2 MPa.

Table 2: Parameters of the gas desorption velocity.

Positive pressure (MPa)	Sorption equilibrium pressures (MPa)	V_a	k	R^2
0	1	0.4503	0.9926	0.96001
	2	0.5529	0.9081	0.97970
	3	0.9853	0.9568	0.95796
	4	1.0893	0.9358	0.94653
0.2	1	0.0311	0.4976	0.96126
	2	0.2162	0.7895	0.97242
	3	0.2700	0.7501	0.98081
	4	0.5824	0.8446	0.96818

small adsorption of helium onto the coal, the correction method was applied according to the positive pressure desorption experiment steps. The free gas content contained in the total gas desorption content can be obtained using helium as the inflation medium.

Thus, the positive pressure gas desorption content is the difference between the gas desorption content and the discharged helium content under the standard state.

$$Q_t = Q - Q_{\text{he}}, \tag{2}$$

where Q_t is the positive pressure gas desorption content andQ_{he} is helium used as the charging medium, and the discharged helium is obtained according to the positive pressure desorption experiment steps.

2.4. Desorption Data Processing Method. The gas desorption velocity was calculated using the following equation:

$$V_{t_2} = \frac{Q_{t_2} - Q_{t_1}}{t_2 - t_1}, \tag{3}$$

where V_{t_2} is the gas desorption velocity at t_2, Q_{t_1} is the gas desorption content at t_1, and Q_{t_2} is the gas desorption content at t_2.

The Winter equation (Equation (4)) was used to fit and analyze the gas desorption velocity, and the relationship between the gas desorption speed and desorption time and the initial gas desorption velocity was obtained.

$$V_t = V_a t^{-k}, \tag{4}$$

where V_t is the gas desorption velocity at t; V_a is theoretically equal to the gas desorption velocity in the first second, that is, the initial gas desorption velocity; and k represents the fitting parameters.

The Uskinov equation (Equation (5)) can be used to describe the gas desorption curve, which shows the initial gas desorption velocity of the sample.

$$Q_t = v_0 \left[\frac{(1+t)^{1-n} - 1}{1-n}\right], \tag{5}$$

where v_0 is the initial gas desorption velocity and n is the fitting parameter.

3. Results

3.1. Desorption Velocity under Different Adsorption Equilibrium Pressures. Figure 3 shows the relationship between the desorption velocity and time for the Sihe sample a particle size of 1–3 mm under pressures of 1 MPa, 2 MPa, 3 MP, and 4 MPa, a temperature of 20°C, and different environmental pressures (atmospheric pressure and 0.2 MPa). Table 2 presents the parameters of the gas desorption velocity obtained using Equation (4).

Figure 3 shows that the variations in the gas desorption velocity of the Sihe coal sample with desorption time obey a power function distribution. After the desorption begins, the gas desorption velocity of the coal sample decreases to varying degrees. At the beginning of the desorption, the gas desorption velocity decreases greatly with increasing desorption time. As the desorption time increases, the reduction range of the gas desorption velocity decreases and gradually approaches zero. Table 2 shows that the initial gas desorption velocity of the coal sample exhibits the same change trend as the adsorption equilibrium pressure under the atmospheric and positive pressure environments, and the initial gas desorption velocity V_a increases monotonously as the adsorption equilibrium pressure increases.

3.2. Desorption Velocity under Different Positive Pressures. Figure 4 shows the relationship between the desorption content and time based on the Uskinov equation (Equation (5)). Table 3 presents the parameters of the gas desorption content obtained using Equation (5).

Table 3 shows that under an ambient temperature of 30°C, the initial gas desorption velocity of the coal sample decreased gradually with increasing positive pressure. Compared with atmospheric pressure desorption, the initial gas desorption speeds under 0.2 MPa, 0.5 MPa, 1 MPa, and 1.5 MPa were 28.29%, 52.13%, 59.58%, and 74.49% lower, respectively. Under an ambient temperature of 20°C, compared with atmospheric pressure desorption, the initial gas desorption velocities under 0.2 MPa, 0.5 MPa, 1 MPa, and 1.5 MPa were 18.48%, 20.82%, 25.88%, and 45.71% lower, respectively. These data demonstrate that the positive pressure effectively inhibited the initial gas desorption velocity. During the actual ARCS process, when the sampling bit breaks the coal, the bottom hole is in a high positive pressure environment, which has a strong inhibitory effect on the desorption from the coal samples. The coal sample returns with the high-speed gas flow, the environmental pressure of the coal sample decreases, the maximum amount of gas desorption and the initial gas desorption speed of the coal sample increase rapidly, and the inhibitory effect of the environmental pressure on the gas desorption decreases.

3.3. Variations in Desorption Velocity with Particle Size. Figure 5 shows the relationship between the desorption content and time for the Sihe coal samples with different particle

sizes under positive pressures of 0.5 MPa and 1 MPa obtained using the Uskinov equation (Equation (5)). Table 4 shows the parameters of the gas desorption content obtained using Equation (5).

Table 4 shows that the initial gas desorption velocity decreased as the coal particle size increases under a given positive desorption pressure. The initial gas desorption rate of the coal sample decreased obviously when the coal particle size increased from the millimeter to centimeter scale. The initial gas desorption rate of the centimeter-size coal sample decreased slightly with increasing particle size. During the actual reverse circulation sampling process, when the sampling bit breaks the coal, the particle size of the sample is large and the initial gas desorption speed is small. The coal sample returns with the high-speed gas flow, the particle size of the coal sample decreases through collisions, and the initial desorption velocity of the coal sample increases.

3.4. Discussion of Sample Desorption Curve during ARCS. Based on the variation characteristics of the initial gas desorption velocity of the coal samples with different particle sizes under different positive pressures, the entire sample desorption process can be divided into three stages (Figure 6): a slow desorption stage, an accelerated desorption stage, and an atmospheric desorption stage. The coal sample is near the bottom of the hole in the slow desorption stage. In this stage, the desorption of the coal sample is slow because the desorption of the large particle size coal sample is inhibited under the positive pressure environment of the bottom of the hole. The accelerated desorption stage refers to the accelerated upward return process of the coal sample in the well. Due to the decrease in the environmental pressure and the decrease in the particle size of the coal sample via collisions during the upward return process, the desorption velocity of the coal sample increases rapidly. The atmospheric desorption stage refers to the atmospheric desorption of the coal sample after reaching the ground surface.

4. Numerical Model

4.1. Diffusion Coefficient. The gas diffusion coefficient is a basic parameter used to characterize the gas desorption and diffusion in coal. The gas diffusion coefficient must be determined to establish a gas diffusion model. The gas diffusion coefficient can be calculated using the following equations [22]:

$$\ln\left(1-\frac{Q_t}{Q_\infty}\right) = -\lambda t + \ln A, \tag{6}$$

$$\lambda = {\beta_1}^2 \frac{D}{{r_0}^2}, \tag{7}$$

$$A = \frac{6(\beta_1 \cos\beta_1 - \sin\beta_1)^2}{{\beta_1}^2\left({\beta_1}^2 - \beta_1 \sin\beta_1 \cos\beta_1\right)}, \tag{8}$$

where Q_∞ is the limit of the gas desorption content, which is calculated using Equation (9), $-\lambda$ and A are fitting parameters, D is the gas diffusion coefficient, and r_0 is the coal particle radius.

$$Q_\infty = \frac{abP}{1+bP} \cdot \frac{1}{1+0.31M_{ad}} \cdot \frac{100 - A_{ad} - M_{ad}}{100}, \tag{9}$$

where a and b are the Langmuir adsorption constants, P is the sorption equilibrium pressure, M_{ad} is the moisture content of the coal sample, and A_{ad} is the ash content of the coal sample.

In the rectangular coordinate system, t was taken as the abscissa, $\ln(1 - Qt/Q_\infty)$ was taken as the ordinate, and λ and A were calculated, and the calculation results were substituted into Equation (7) to obtain the diffusion coefficient D. Figure 7 shows the relationship between $\ln(1 - Qt/Q_\infty)$ and t. Table 5 shows the calculation results for λ, A, and D. It can be seen from the table that the diffusion coefficient decreases with increasing positive pressure for a given adsorption equilibrium pressure. To use the gas diffusion model to predict the gas desorption curve under different positive pressure conditions, it is necessary to determine the relationship between the positive pressure and diffusion coefficient. The fitting of the positive pressure and diffusion coefficient data (Figure 8) shows that the relationship between the positive pressure and diffusion coefficient conforms to

$$D = A_1 e^{(-P/A_2)} + A_3, \tag{10}$$

where p is the positive pressure and A_1, A_2, and A_3 are the fitting parameters.

4.2. Model Establishment. Gas desorption from coal particles is a complex process. From the point of view of molecular motion, the adsorption and desorption of the gas molecules onto and from the pore walls are completed instantaneously. However, in fact, the flow of gas through granular coal takes a certain amount of time because the resistance needs to be overcome when the gas gushes from the granular coal through pores and fractures of different sizes. The emission process of the gas from the granular coal is regarded as the diffusion of gas in a porous media, and its emission law conforms to Fick's law of diffusion:

$$J = -D\frac{\partial C}{\partial x}, \tag{11}$$

where J is the diffusion velocity of the diffusing fluid passing through a unit area, $\partial C/\partial x$ is the concentration gradient along the diffusion direction, and C is the concentration of the diffusing fluid.

This equation is the first law of diffusion. In Equation (11), the negative sign indicates that diffusion occurs in the opposite direction of the concentration increase. When Fick's law of diffusion is applied to a three-dimensional unsteady flow field, the second law of diffusion can be derived according to the law of mass conservation and the

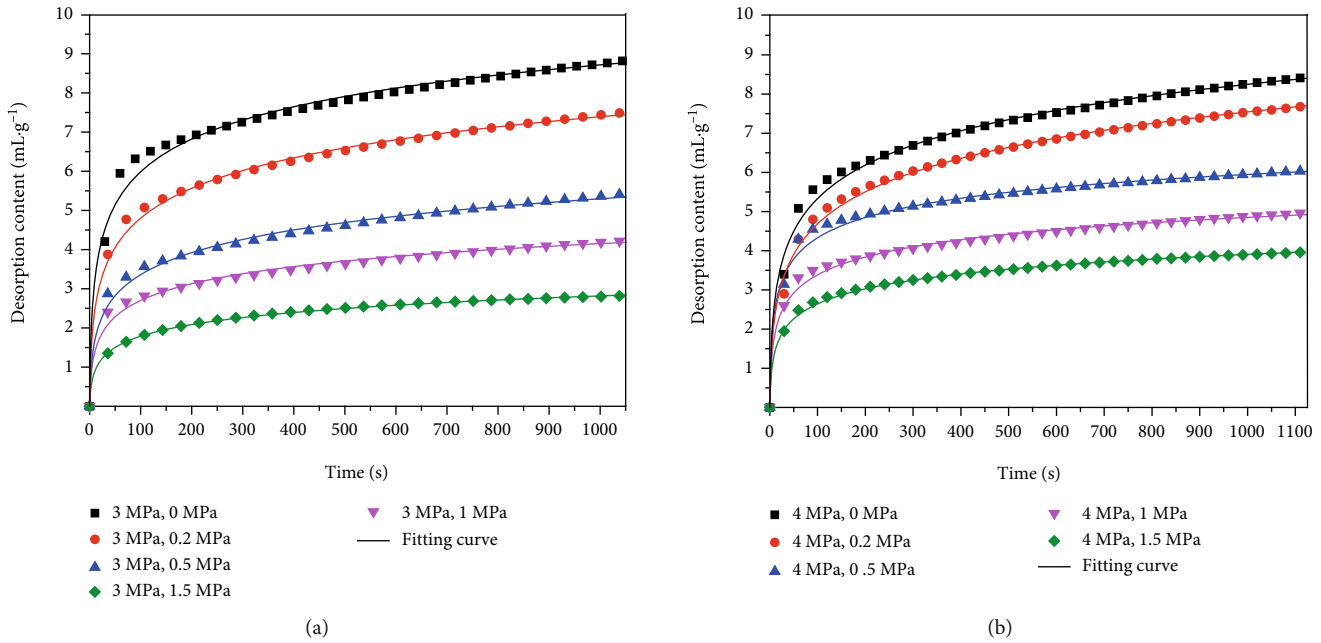

Figure 4: Relationship between the desorption content and time under different positive pressures: (a) Sihe sample and (b) Canghai sample.

Table 3: Parameters of gas desorption content.

Sample	Temperature (°C) Sorption equilibrium pressure (MPa) Positive pressure (MPa)	Initial gas desorption velocity (mL/(g·s))	Fitting parameter	R^2
Sihe	30-3-0	$v_0 = 1.3702$	$n = 1.0246$	0.96309
	30-3-0.2	$v_0 = 0.9826$	$n = 0.9759$	0.98212
	30-3-0.5	$v_0 = 0.6559$	$n = 0.9562$	0.98318
	30-3-1	$v_0 = 0.5539$	$n = 0.9769$	0.98135
	30-3-1.5	$v_0 = 0.3495$	$n = 0.9567$	0.99003
Canghai	20-4-0	$v_0 = 1.0819$	$n = 0.9719$	0.97619
	20-4-0.2	$v_0 = 0.8820$	$n = 0.9401$	0.98137
	20-4-0.5	$v_0 = 0.8567$	$n = 0.9815$	0.97595
	20-4-1	$v_0 = 0.8019$	$n = 1.0393$	0.97640
	20-4-1.5	$v_0 = 0.5874$	$n = 1.0110$	0.97931

principle of continuity:

$$\frac{\partial c}{\partial t} = D\left(\frac{\partial^2 C}{\partial r^2} + \frac{2}{r}\frac{\partial C}{\partial r}\right), \tag{12}$$

where r is the radius.

The model is a classical homogeneous coal particle diffusion model, and its assumptions are as follows: (1) the coal chips are composed of spherical particles. (2) The coal cuttings are homogeneous and isotropic. (3) The gas flow follows the law of mass conservation and the principle of continuity. (4) The diffusion coefficient is independent of the concentration, time, and coordinates. (5) The gas desorption from the coal dust is an isobaric desorption process under isothermal conditions.

The mathematical method is used to discuss the theoretical solution of the equation for gas diffusion from coal dust. Set $u = Cr$, and substitute it into Equation (12) to obtain

$$\frac{\partial u}{\partial t} = D\frac{\partial^2 u}{\partial r^2}. \tag{13}$$

Thus, the coal gas diffusion equation is changed into a one-dimensional linear flow equation. For coal particles, the concentration reaches a certain value C_0 when adsorption equilibrium is reached. The gas concentration on the coal particle surfaces decreases (the adsorbed gas on the coal

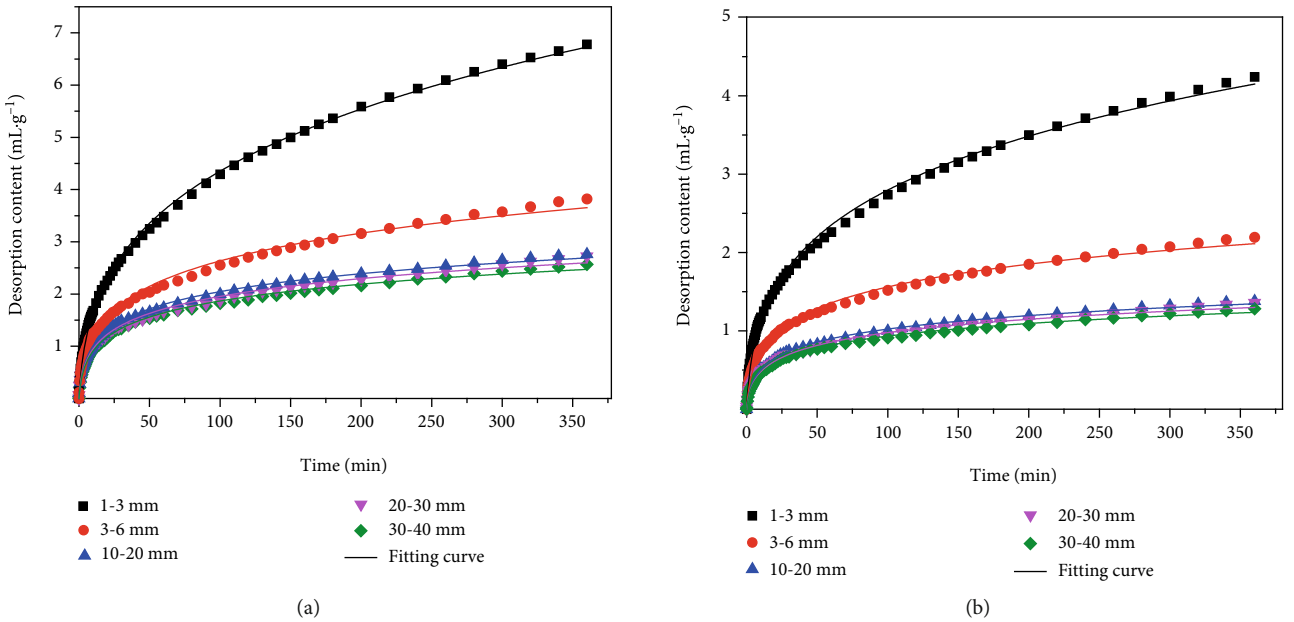

Figure 5: Relationship between the desorption content and time for different particle sizes: (a) positive pressure of 0.5 MPa and (b) positive pressure of 1 MPa.

Table 4: Parameters of gas desorption content.

Sample	Temperature (°C) Sorption equilibrium pressure (MPa) Particle size (mm) Positive pressure (MPa)	Initial gas desorption velocity (mL·g^{-1}·s^{-1}) v_0	Fitting parameter n	R^2
Sihe	30-2-1-3-0.5	$v_0 = 0.5027$	$n = 0.7510$	99.803
	30-2-3-6-0.5	$v_0 = 0.4284$	$n = 0.8812$	99.204
	30-2-10-20-0.5	$v_0 = 0.3980$	$n = 0.9542$	99.636
	30-2-20-30-0.5	$v_0 = 0.3666$	$n = 0.9390$	99.488
	30-2-30-40-0.5	$v_0 = 0.3547$	$n = 0.9444$	99.729
	30-2-1-3-1	$v_0 = 0.3668$	$n = 0.7980$	99.632
	30-2-3-6-1	$v_0 = 0.2748$	$n = 0.9131$	99.419
	30-2-10-20-1	$v_0 = 0.1990$	$n = 0.9541$	99.636
	30-2-20-30-1	$v_0 = 0.1833$	$n = 0.9389$	99.488
	30-2-30-40-1	$v_0 = 0.1773$	$n = 0.9443$	99.729

particle surfaces is equal to the adsorbed gas under positive pressure) when the coal particles are suddenly exposed to a certain positive pressure. At this time, a concentration difference is formed along the direction of the radius of the coal particles, and the adsorbed gas changes to a free state, resulting in the diffusion of gas from the center of the coal particles to the surface. The surface concentration is constant C_1. At this time, the initial and boundary conditions are as follows:

$$\frac{\partial u}{\partial t} = D\frac{\partial^2 u}{\partial r^2} \quad (0 < r < r_0, t > 0), \tag{14}$$

$$u = 0 \quad (r = 0, t > 0), \tag{15}$$

$$u = r_0 C_1 \quad (r = r_0, t > 0), \tag{16}$$

$$u = rC_0 \quad (0 < r < r_0, t = 0), \tag{17}$$

where r_0 is the radius of the coal particles.

By solving Equation (14), the relationship between the gas concentration in the coal particles and time can be

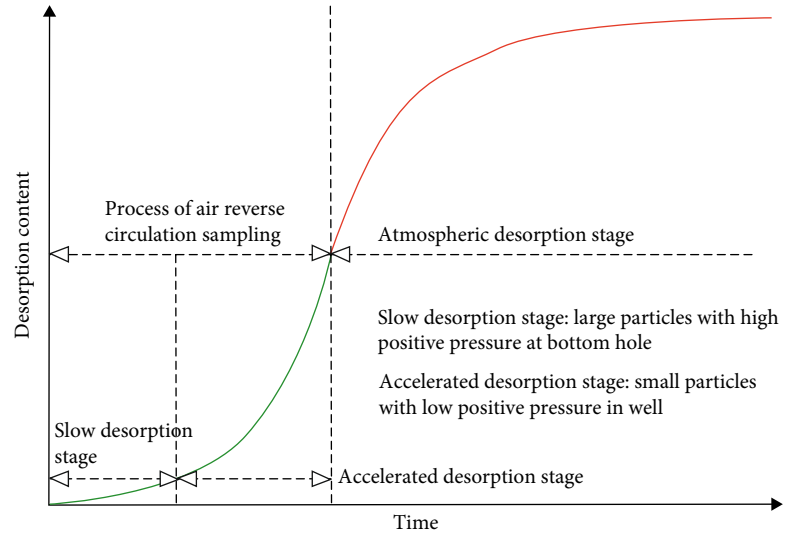

Figure 6: Sample desorption curve during ARCS.

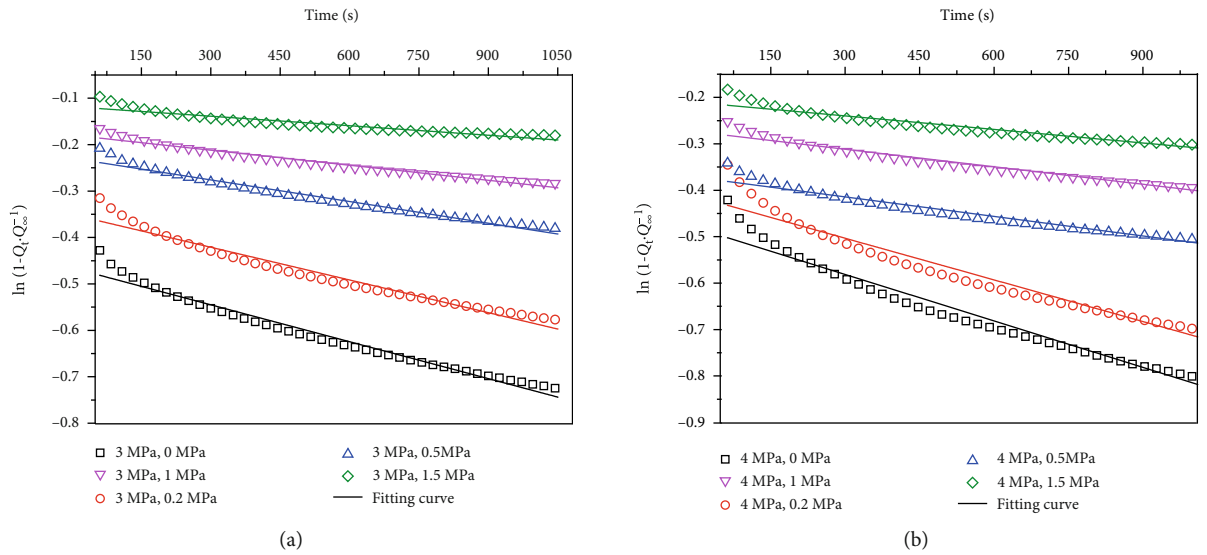

Figure 7: Relationship between $\ln(1 - Q_t/Q_\infty)$ and t: (a) Sihe sample and (b) Canghai sample.

obtained:

$$C(r,t) = C_1 + (C_0 - C_1)\frac{2r_0}{\pi r}\sum_{n=1}^{\infty}\left[\frac{(-1)^{n+1}}{n}e^{-(n\pi/r_0)^2 Dt}\sin\frac{n\pi r}{r_0}\right], \tag{18}$$

where C_1 is the surface concentration of the coal particles, $C_1 = abp/(1+bp)$, and C_0 is the initial concentration of the coal particles, $C_0 = abP/(1+bP)$.

$C(r,t)$ is the expression of the gas concentration distribution in the coal particles under positive pressure. By integrating B in the spherical coordinate system, the expression of the amount of desorption with time can be obtained:

$$Q_t = \frac{8}{\pi}{r_0}^3(C_1 - C_0)\sum_{n=1}^{\infty}\frac{1}{n^2}e^{-(n\pi/r_0)^2 Dt} + \frac{4\pi{r_0}^3}{3}(C_0 - C_1). \tag{19}$$

4.3. Numerical Solution of the Theoretical Model. The diffusion coefficients of the Sihe coal particles under a pressure of 3 MPa, a temperature of 30°C, and positive pressures of 0.3 MPa, 0.8 MPa, 1.2 MPa, and 2 MPa and that of the Canghai coal particles under a pressure of 4 MPa, a temperature of 20°C, and positive pressures 0.3 MPa, 0.8 MPa, 1.2 MPa, and 2 MPa were predicted using Equation (10). The numerical solutions of $C(r,t)$ and Q_t were determined using

Table 5: Calculation results for λ, A, and D.

Sample	Temperature (°C) Sorption equilibrium pressure (MPa) Positive pressure (MPa)	λ	A	D (mm^2/s)
Sihe	30-3-0	2.65053×10^{-4}	0.62757	6.17699×10^{-11}
	30-3-0.2	2.14933×10^{-4}	0.704336	5.51506×10^{-11}
	30-3-0.5	1.5514×10^{-4}	0.795106	4.61977×10^{-11}
	30-3-1	1.08019×10^{-4}	0.835663	3.51509×10^{-11}
	30-3-1.5	6.83205×10^{-5}	0.888474	2.60028×10^{-11}
Canghai	20-4-0	3.33583×10^{-4}	0.617992	7.69018×10^{-11}
	20-4-0.2	2.69079×10^{-4}	0.661265	6.52619×10^{-11}
	20-4-0.5	1.80213×10^{-4}	0.689216	4.53066×10^{-11}
	20-4-1	1.25799×10^{-4}	0.760401	3.51724×10^{-11}
	20-4-1.5	9.7248×10^{-5}	0.810082	2.98598×10^{-11}

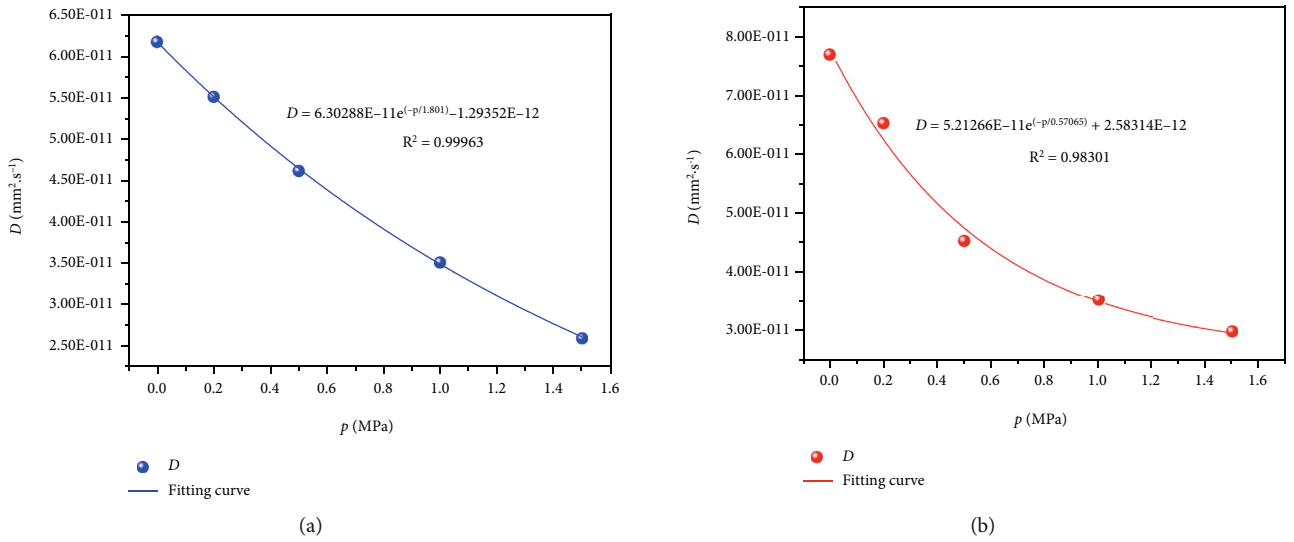

Figure 8: The fitting of the positive pressure and diffusion coefficient data: (a) Sihe sample and (b) Canghai sample.

Table 6: Numerical solution parameters.

Sample	Temperature (°C) Sorption equilibrium pressure (MPa) Positive pressure (MPa)	D (m^2/s)	t_1 (s)	t_2 (s)	a	b	d (mm)
Sihe	30-3-0.3	5.46512×10^{-11}	600	1000	35.8597	1.6663	0.728
	30-3-0.8	4.17163×10^{-11}					
	30-3-1.2	3.36656×10^{-11}					
	30-3-2	2.2055×10^{-11}					
Canghai	20-4-0.3	5.66451×10^{-11}			30.7046	1.362	0.706
	20-4-0.8	3.86611×10^{-11}					
	20-4-1.2	3.21964×10^{-11}					
	20-4-2	2.7398×10^{-11}					

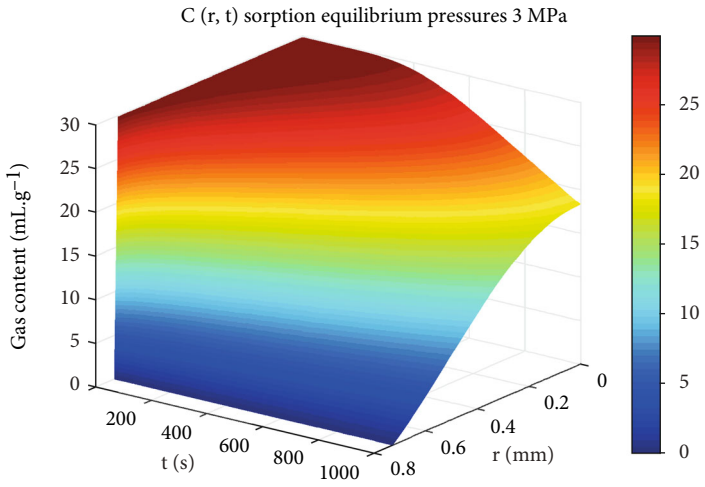

(a) Sihe sample, positive pressure of 0 MPa, desorption time of 1000 s

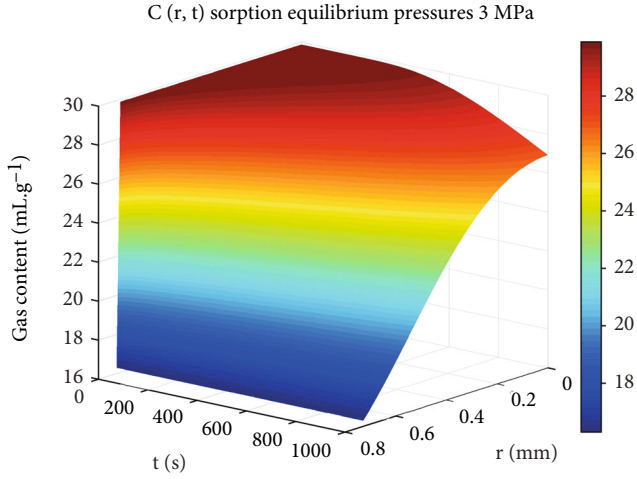

(b) Sihe sample, positive pressure of 0.5 MPa, desorption time of 1000 s

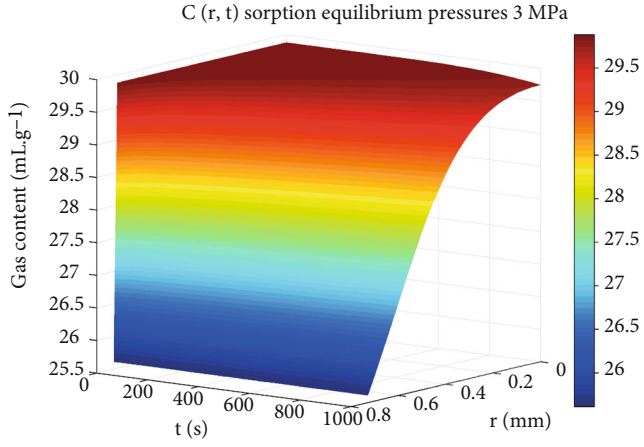

(c) Sihe sample, positive pressure of 1.5 MPa, desorption time of 1000 s

Figure 9: Continued.

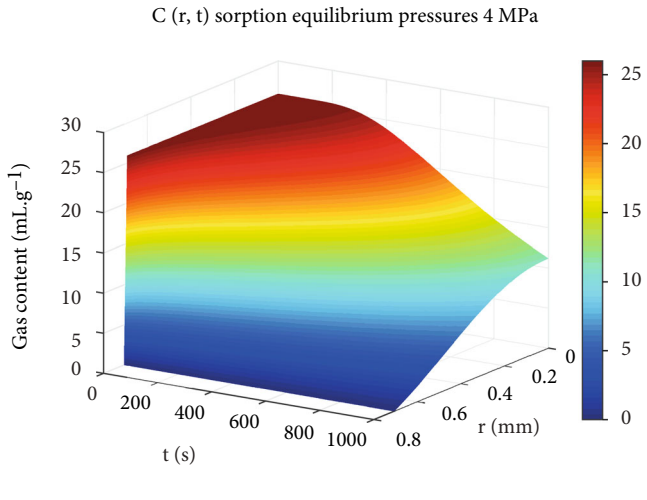

(d) Canghai sample, positive pressure of 0 MPa, desorption time of 1000 s

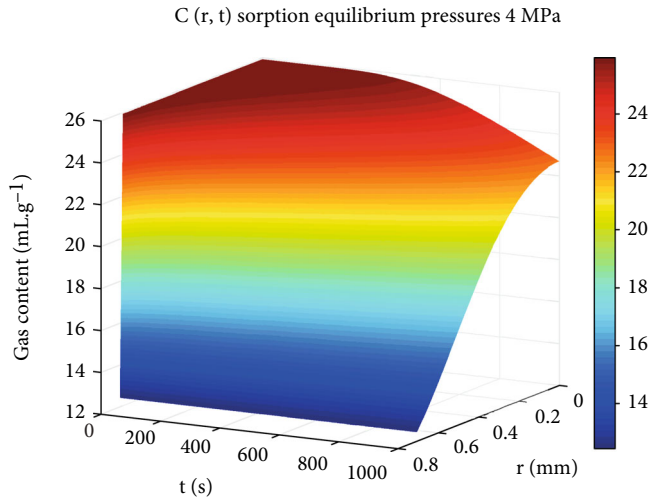

(e) Canghai sample, positive pressure of 0.5 MPa, desorption time of 1000 s

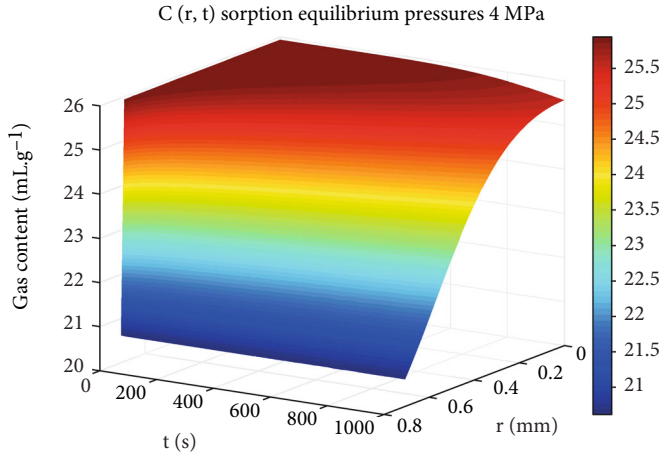

(f) Canghai sample, positive pressure of 1.5 MPa, desorption time of 1000 s

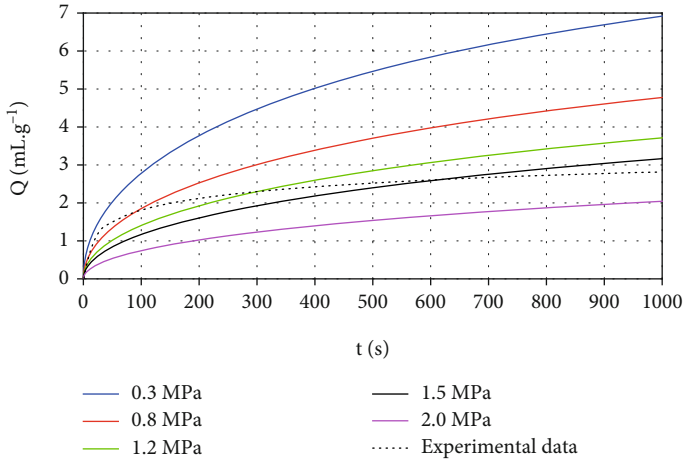

(g) Predictions of gas desorption content of Sihe sample

Figure 9: Continued.

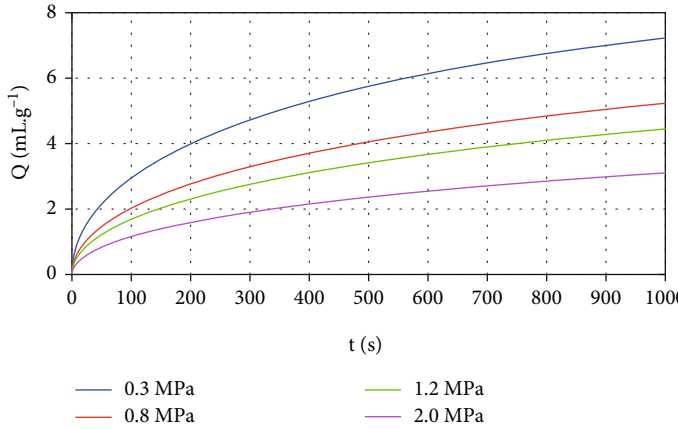

(h) Predictions of gas desorption content of Canghai sample

Figure 9: Results of numerical solution.

MATLAB. The numerical solution parameters are presented in Table 6. Figure 9 shows the results of the numerical solution.

Figures 9(a)–9(f) show the distribution of the gas content of the coal particles. The figures show that the gas content of the spherical coal particles gradually decreases from the center of the particle to the surface, with the maximum content at the ball's center and the minimum gas content on the surface. The gas content in the coal particles gradually decreases as the desorption time increases. The gas content at the center of the ball decreases slightly, and the gas content near the surface of the ball decreases greatly. The gas content of the coal body decreases significantly within 1000 s, and the gas content at the ball's center decreases significantly when the ambient desorption pressure is the atmospheric pressure. The gas content of the coal body decreases obviously from the center of the particle toward the surface within 1000 s, and it decreases slightly at the ball's center when the positive pressure of the desorption environment reaches 0.5 MPa. The gas content of the coal body near the sphere's surface decreases obviously within 1000 s, and the gas content at the sphere's center decreases slowly when the positive pressure of the desorption environment reaches 1.5 MPa. This shows that positive pressure can effectively inhibit the desorption of gas from coal.

Figures 9(g) and 9(h) show the prediction curves of the gas desorption contents of the Sihe and Canghai coal samples under positive pressures of 0.3 MPa, 0.8 MPa, 1.2 MPa, and 2 MPa. In addition, the prediction curve of the gas desorption capacity at 1.5 MPa for the Sihe coal sample and the experimental data curve are presented in Figure 9(g). The desorption trends of the two are basically consistent. The predicted desorption capacity at 1000 s is 3.1654 mL/g, and the experimentally measured desorption capacity at 1000 s is 2.8104 mL/g, with an error of 12.6%. The predicted gas desorption capacities at 1000 s for the Sihe coal sample under positive pressures of 0.3 MPa, 0.8 MPa, 1.2 MPa, 1.5 MPa, and 2 MPa are 6.919 mL/g, 4.7762 mL/g, 3.7137 mL/g, 3.1654 mL/g, and 2.0436 mL/g, respectively. The gas contents of the Canghai coal sample under positive pressures of 0.3 MPa, 0.8 MPa, 1.2 MPa, and 2 MPa are 7.2286 mL/g, 5.2339 mL/g, 4.4475 mL/g, and 3.1046 mL g, respectively.

5. Conclusions

(1) The response characteristics of positive pressure desorption and atmospheric pressure desorption to the adsorption equilibrium pressure are similar. For a given desorption positive pressure, the gas desorption velocity increases as the adsorption equilibrium pressure increases

(2) Positive pressure can effectively inhibit gas desorption. For a given desorption positive pressure, the initial gas desorption velocity decreases as the positive pressure increases; and the initial gas desorption velocity decreases as the coal particle size increases. Moreover, the entire sample desorption during the ARCS process can be divided into three stages

(3) The diffusion coefficients of the Sihe and Canghai coal samples under different positive pressures were calculated, and the relationship between the diffusion coefficient and positive pressure was found to obey an exponential distribution

(4) The positive pressure diffusion model can describe the gas diffusion from coal particles well using the diffusion coefficients calculated based on the results of the experiments. The gas diffusion contents under positive pressures of 0.3 MPa, 0.8 MPa, 1.2 MPa, and 2 MPa were simulated

Data Availability

When other researchers need data, the author can provide it.

Conflicts of Interest

The author declares no competing financial interest.

Acknowledgments

The author acknowledges the relevant coal mine for providing the desired coal samples for this study. This work was supported by the National Key Research and Development Program of China (2018YFC0808001).

References

[1] Y. P. Cheng, H. N. Jiang, X. L. Zhang, J. Cui, C. Song, and X. Li, "Effects of coal rank on physicochemical properties of coal and on methane adsorption," *International Journal of Coal Science and Technology*, vol. 4, no. 2, pp. 129–146, 2017.

[2] Y. Li, S. Q. Pan, S. Z. Ning, L. Shao, Z. Jing, and Z. Wang, "Coal measure metallogeny: metallogenic system and implication for resource and environment," *Science China Earth Sciences*, vol. 65, no. 7, pp. 1211–1228, 2022.

[3] Z. F. Wang, X. Tang, G. W. Yue, B. Kang, C. Xie, and X. Li, "Physical simulation of temperature influence on methane sorption and kinetics in coal: benefits of temperature under 273.15 K," *Fuel*, vol. 158, pp. 207–216, 2015.

[4] S. Tao, Z. J. Pan, S. L. Tang, and S. Chen, "Current status and geological conditions for the applicability of CBM drilling technologies in China: a review," *International Journal of Coal Geology*, vol. 202, pp. 95–108, 2019.

[5] Y. Li, Z. S. Wang, S. H. Tang, and D. Elsworth, "Re-evaluating adsorbed and free methane content in coal and its ad- and desorption processes analysis," *Chemical Engineering Journal*, vol. 428, article 131946, 2022.

[6] Y. Qin, "The situation and challenges faced by the industrialization of coalbed methane in China (I) -the current stage of development," *Natural Gas Industry*, vol. 26, no. 1, pp. 4–7, 2006.

[7] R. M. Barrer, *Diffusion in and through Solids*, The University Press, New York, 1941.

[8] P. G. Sevenster, "Diffusion of gases from coal," *Fuel*, vol. 38, no. 6, pp. 403–418, 1959.

[9] K. Winter and H. Janas, *Gas emission characteristics of coal and methods of determining the desorbable gas content by means of desorbometers*, Proceedings of the 14th international conference of coal mine safety research, 1996.

[10] Q. F. Yang and Y. A. Wang, "Theory and application of coal dust gas diffusion," *Journal of China Coal Society*, vol. 3, pp. 87–94, 1986.

[11] S. P. Nandi and P. L. Walker, "Activated diffusion of methane from coals at elevated pressures," *Fuel*, vol. 54, no. 2, pp. 81–86, 1975.

[12] L. M. Knox and J. Hadro, "Canister desorption techniques-variations and reliability," *Proceedings, International Coalbed Methane Symposium*, pp. 319–329, Tuscaloosa, Alabama, 2001.

[13] J. S. Wang, *Design and experimental study of DTH Reverse Circulation Bit for fast drilling*, Jilin University, Jilin, China, 2015, Doctoral Dissertation,.

[14] D. M. Chen, W. Long, Y. Y. Li, and R. Zhang, "Study on change rules of factors affecting gas loss during coalbed air reverse circulation sampling," *Advances in Civil Engineering*, vol. 2021, Article ID 5550726, 15 pages, 2021.

[15] Y. Li, C. Zhang, D. Tang et al., "Coal pore size distributions controlled by the coalification process: an experimental study of coals from the Junggar, Ordos and Qinshui basins in China," *Fuel*, vol. 206, pp. 352–363, 2017.

[16] S. Tao, Y. B. Wang, D. Z. Tang et al., "Dynamic variation effects of coal permeability during the coalbed methane development process in the Qinshui Basin, China," *International Journal of Coal Geology*, vol. 93, pp. 16–22, 2012.

[17] X. Chen, Z. Duan, L. Yang, and W. Peng, "Experiment study on diffusion features of gassy coal under negative pressure environment," *Coal Science and Technology*, vol. 51, no. 10, pp. 191–195, 2020.

[18] H. T. Zhang, Y. S. Hao, and J. P. Wei, "Study on characteristic parameters of particulate coal gas desorption and diffusion under negative pressure environment," *Safety in Coal Mines*, vol. 51, no. 10, pp. 191–195, 2020.

[19] Z. B. Yang, Y. Qin, Z. F. Wang, G. Wang, and C. F. Wu, "Desorption-diffusion model and lost gas quantity estimation of coalbed methane from coal core under drilling fluid medium," *Science China Earth Sciences*, vol. 53, no. 4, pp. 626–632, 2010.

[20] B. Nie, T. Yang, X. Li, L. Li, and H. Lu, "Research on diffusion of methane in coal particles," *Journal of China University of Mining and Technology*, vol. 42, no. 6, pp. 978–981, 2013.

[21] N. Brook, "A modified method of determining the Protodyakonov number, and its correlation with compressive strength," *International Society Rock Mech*, vol. 1, pp. 1–19, 1970.

[22] B. Nie, Y. Guo, S. Wu, and L. Zhang, "Theoretical model and analytical solution of coal particle gas diffusion," *Journal of China University of Mining and Technology*, vol. 1, pp. 21–24, 2001.